Discovery of an essential mycobacterial polar growth factor involved in cell envelope integrity and lipomannan and lipoarabinomannan transport

Kuldeepkumar R. Gupta[a], Kathryn C. Rahlwes[b], Chunyan Wang[c], Jun Liu[c], Yasu S. Morita[b], and E. Hesper Rego[a,1]

[a]Department of Microbial Pathogenesis, Yale University School of Medicine, New Haven, CT 06519

[b]Department of Microbiology, University of Massachusetts, Amherst, MA 01003

[c]Department of Microbial Pathogenesis, Microbial Sciences Institute, Yale University School of Medicine, New Haven, CT, USA 06519

[1]To whom correspondence should be addressed: hesper.rego@yale.edu

ABSTRACT

Mycobacteria grow and divide differently compared to well-studied model bacteria. They insert new cell envelope at their poles instead of along their side walls; and, they lack obvious homologs of many well-conserved cell growth and division proteins. Furthermore, while mycobacteria share several similarities to Gram-positive bacteria, unlike these organisms they possess an outer membrane, which is abundant in long-chain fatty acids and several glycolipids and lipoglycans. A better understanding of the unique factors that make this unusual structure could lead to therapeutic targets for pathogenic mycobacteria. Here, we study a gene of previously unknown function – *msmeg_0317* - predicted to be essential and associated with mycobacterial cell growth and division proteins. We find that transcriptional depletion of *msmeg_0317* leads to loss of polar

growth, disruption of the mycobacterial outer membrane, and cell death. Surprisingly, we also observe that depletion results in the accumulation of cell-associated lipoglycans lipomannan and lipoarabinomannan (LM/LAM), while overexpression of CwdA leads to increased shedding of LM/LAM. LM/LAM have been extensively studied in relation to infection but their role in bacterial physiology is less clear. Altogether, our data suggest that MSMEG_0317, renamed CwdA, is involved in the transport of LM/LAM to the mycobacterial outer membrane, and reveal unexpected connections between the correct localization of LM/LAM, polar growth, and the structural integrity of the mycobacterial cell envelope.

IMPORTANCE. Some of the most successful antibiotics target bacterial cell envelope synthesis. However, the cell envelope of mycobacteria is significantly different from that of other, more well-studied, bacteria. Its core structure consists of a covalently-linked network of peptides, carbohydrates, and fatty acids. Additionally, there are several lipids non-covalently interspersed throughout. Many of the enzymes which synthesize these lipids are known, but how they are transported remains largely unclear. Here, we discover that an essential protein, CwdA, is involved in the transport of LM/LAM, abundant lipoglycans in the mycobacterial cell envelope. Depletion of CwdA leads to the loss of polar growth and the disintegration of the mycobacterial outer membrane. These results suggest that the proteins which transport molecules across the mycobacterial cell envelope may represent an abundant source of novel drug targets for the treatment of mycobacterial infections, like tuberculosis.

47 **INTRODUCTION**

48 *Mycobacterium tuberculosis* (Mtb), the etiological agent of human tuberculosis
49 (TB), is responsible for approximately 1.4 million deaths each year. One of the pathogen's
50 distinguishing features is its unusual cell envelope. Like nearly all other bacterial species,
51 the plasma membrane is surrounded by peptidoglycan, a rigid mesh-like structure made
52 up of carbohydrate chains crosslinked by peptide bridges. However, in contrast to the
53 peptidoglycan of other well-characterized bacteria, mycobacterial peptidoglycan is
54 covalently linked to the highly branched hetero-polysaccharide arabinogalactan, which is,
55 itself, covalently bound to extremely long-chained fatty acids called mycolic acids.
56 Electron microscopy has revealed that the outer cell envelope is a lipid bilayer, and, as
57 such, it is referred to as the outer membrane, or, alternatively, the mycomembrane (1, 2).
58 In addition to this core structure, several lipids are abundantly and non-covalently
59 interspersed across the plasma membrane and outer membrane (3, 4). This complex cell
60 envelope is a double-edged sword: it is a formidable barrier to many antibiotics, yet
61 provides a number of potentially targetable structures. Indeed, two of the four first-line TB
62 antibiotics target cell-envelope biosynthesis.

63 In addition to their unusual cell envelope, mycobacteria differ from other well-
64 studied rod-shaped bacteria in important ways. Notably, mycobacteria elongate from their
65 poles rather than along their side walls. The details of polar growth are poorly understood
66 (5-7). Many key proteins important for cell elongation in other species appear to be
67 missing in mycobacteria (6, 8). Likewise, it is almost completely unknown how proteins
68 involved in synthesizing the different layers, and free lipids, work together to build this
69 complex cell envelope.

70 Given the unusual physiology of mycobacteria, perhaps it is unsurprising that
71 greater than 25% of the genes encoded by the mycobacterial genome are annotated as
72 having unknown function (9). In our previous studies on the mycobacterial division
73 complex, 'the divisome', we precipitated known divisome and elongasome components
74 from *M. smegmatis* (Msm), and identified multiple candidate mycobacterial-specific
75 divisome proteins in the precipitate, (8, 10). One of these was MSMEG_0317, a protein
76 of unknown function that is highly conserved in actinobacteria. The Mtb homolog of
77 *msmeg_0317*, *rv0227c*, is predicted to be essential (11, 12). Here, we sought to
78 understand the role of MSMEG_0317 during mycobacterial growth and division.

79 MSMEG_0317 belongs to the DUF3068-domain super-family of proteins, which
80 are exclusively found in actinobacteria. One member of this family in corynebacteria has
81 channel activity, so this domain has been renamed PorA (13, 14). In addition, by structure-
82 based homology prediction, MSMEG_0317 shares limited homology to mycobacterial
83 lipoproteins, LppX and LrpG, which transport lipids, phthiocerol dimycocerosates (PDIMs)
84 and triacylglycerol (TAG), respectively, to the outer mycobacterial membrane (15, 16).

85 We find that MSMEG_0317 localizes to sites of new cell wall synthesis and is
86 indeed essential for cell viability in Msm. Transcriptional depletion leads to loss of cellular
87 elongation, reductive division, and eventually cell lysis. Surprisingly, we find that
88 lipomannan (LM), and lipoarabinomannan (LAM) – two large lipoglycans abundant in the
89 mycobacterial cell envelope - accumulate as MSMEG_0317 is depleted and are shed into
90 the culture media more abundantly upon MSMEG_0317 overexpression. By cryo-electron
91 microscopy, we find that the cell envelopes of depleted cells are devoid of outer
92 membrane and are highly disrupted. Together, these results show that MSMEG_0317

93 plays an important role in LM/LAM transport to the outer membrane, polar elongation,
94 and the structural organization of the mycobacterial cell wall. As such, we propose to
95 rename *msmeg_0317*, *cwdA*, for cell wall disruption, mutant A.
96
97 **RESULTS**
98 ***cwdA* is essential for polar growth**
99 To determine the essentiality of *cwdA*, we used an allele swapping strategy (17).
100 Briefly, in a strain of Msm whose only copy of *cwdA* was at the L5 phage integration site
101 (18), we exchanged *cwdA* for either an empty vector or for another copy of itself (Fig. 1A).
102 Consistent with *cwdA* being essential for cell growth, we observed approximately 1000-
103 fold fewer colonies when we exchanged *cwdA* with an empty vector compared to
104 exchanging it for another copy of itself (Fig. 1A).
105 To further confirm the essentially of *cwdA*, we constructed a strain in which the
106 only copy of the gene was tetracycline inducible (Fig. 1B). Removal of anhydrotetracycline
107 (ATC) from the culture media prevented cell growth (Fig. 1B). By time-lapse microscopy
108 we observed that, while cells expressing CwdA became longer, on average, as cell
109 density increased within the microfluidic device (Fig. 2A,C & Movie S1), cells depleted for
110 CwdA stopped elongating but continued to divide (reductive division), became wider, and,
111 in many instances, eventually lysed (Fig. 2B,C & Movie S2). Together these data show
112 that *cwdA* is essential for polar elongation in Msm.
113
114 **CwdA localizes to the sites of cell wall synthesis**

115 As our data suggested CwdA is important for polar growth, we hypothesized that
116 it would localize to the poles, which are the sites of new cell wall synthesis in
117 mycobacteria. To test this hypothesis, we made a translational fusion to CwdA with mRFP
118 expressed by its native promoter. By allele swapping, we find that *cwdA-mrfp* restores
119 bacterial growth (Fig. S1) and thus encodes a functional *cwdA*. Fluorescence microscopy
120 at a single time-point showed that CwdA-mRFP localizes to mid-cell and to the poles (Fig.
121 3A). In polar growing bacteria, the site of division eventually becomes the site of
122 elongation. Thus, in addition to localizing to the poles, elongation-complex proteins will
123 also localize to the site of division early during the next cell cycle, making it difficult to
124 distinguish true septal localization from static images. To disentangle whether CwdA also
125 localizes to the septum, we visualized CwdA-mRFP by time-lapse microscopy. By
126 constructing kymographs averaged over many cells, we compared the fluorescence
127 probability distribution over the course of the cell cycle to the earliest known markers for
128 the division complex (FtsZ-mCherry2B) and the elongation complex (eGFP-Wag31).
129 CwdA-mRFP localizes to the site of division after FtsZ, but before Wag31 (Fig. 3B). These
130 data are consistent with CwdA being a member of both the mycobacterial division and
131 elongation complexes, but its essential function is as part of the elongation complex.
132
133 **CwdA is involved in LM/LAM transport**
134 The corynebacterial homolog of *cwdA* was recently implicated in LM/LAM
135 biosynthesis (19), as a deletion mutant of the *Corynebacterium glutamicum* homolog
136 resulted in disappearance of LAM and accumulation of truncated LM, which was clearly
137 detectable by faster migration on SDS-PAGE. To test if this is also the case in

138 mycobacteria, we used the same electrophoretic approach to analyze LM/LAM, and thin
139 layer chromatography (TLC) to examine potential changes in other lipid species upon
140 depletion of CwdA, before and after the onset of cell death (Fig. S2B). In contrast to the
141 results obtained in *C. glutamicum*, we observe a dramatic and transient increase in the
142 total amount of cell-associated of LM/LAM during depletion (Figs. 4A & S2A), up until the
143 onset of cell death. There were no obvious changes in the migration of LM/LAM on SDS-
144 PAGE, implying that the impact of CwdA depletion on LM/LAM biosynthesis was minimal.
145 Additionally, other lipids, including the precursor of LM/LAM biosynthesis such as
146 Ac_1PIM_2, showed no reproducible change (Figs. 4B,C & Fig. S2A).

147 These data are not consistent with the proposed biosynthetic function of the
148 corynebacterial CwdA homolog. Instead, the transient increase of LM/LAM prior to cell
149 death suggests a potential role for CwdA in cell envelope trafficking of these lipoglycans.
150 LM/LAM are thought to be embedded in the plasma membrane, and also transported to
151 the outer membrane (20, 21). Furthermore, LM/LAM in the outer membrane are likely to
152 be shed into the extracellular milieu (22-24). Interestingly, sequence-based homology
153 modeling indicated that CwdA shares some homology to LppX and LprG, proteins known
154 to transport lipids from the inner membrane to the outer membrane in mycobacteria.
155 Therefore, we hypothesized that depletion of CwdA results in the transient increase of
156 cell-associated LM/LAM due to the disruption of LM/LAM trafficking. Based on this
157 hypothesis, we reasoned that over-expression of CwdA may facilitate more trafficking,
158 which could deplete cell-associated LM/LAM and increase shedding. To test this, we
159 constructed strains which inducibly expressed CwdA from a multi-copy plasmid.
160 Consistent with our hypothesis, upon induction with ATC we observed less LM/LAM

161 associated with Msm cells (Figs. S3A & S4) and more LAM secreted in the culture
162 supernatant (Fig. S3B). These data suggest a model whereby CwdA is involved, directly
163 or indirectly, in the transport of LM/LAM to the outer membrane of mycobacteria.
164

165 **CwdA is important for cell envelope integrity**

166 Our model predicts that CwdA-depleted cells should have greatly altered cell
167 envelopes. Thus, we visualized the cell envelope of wild type and mutant cells by high
168 resolution cryo-electron microscopy (cryo-EM). As has been previously observed (1, 2),
169 wild type Msm cells exhibit a distinct plasma membrane and outer membrane that is
170 approximately 50-nm thick (Fig. 5A-C). Consistent with our model, we find that cells
171 depleted for CwdA have largely unstructured cell walls, and appear devoid of electron
172 density in the outer membrane (Fig. 5D-F). We also observe dramatic fraying of the outer
173 membrane, and large invaginations of plasma membrane (Fig. 6). Thus, CwdA is
174 important for maintaining the structural organization of the mycobacterial cell envelope.

175 Collectively, our data show that CwdA is an essential polar growth factor involved
176 in transporting, either directly or indirectly, LM/LAM to the outer membrane. Further, our
177 data suggest that the correct localization of LM/LAM is important for the structural
178 organization and integrity of the mycobacterial cell envelope.
179

180 **DISCUSSION**

181 The extraordinary diversity of the bacterial kingdom has led to a plethora of
182 bacterial cell shapes and geometries of cell growth and division. Unlike well-studied
183 model bacteria, several organisms, including the major human pathogen *Mycobacterium*

184 *tuberculosis,* grow from their poles rather than their side-walls. Our understanding of polar
185 growth is at a nascent stage compared to our knowledge of side-wall growth.
186 Mycobacteria, and related organisms, have an additional challenge of orchestrating the
187 biosynthesis and transport of several additional covalently and non-covalently attached
188 lipids and glycans to their thick layer of peptidoglycan. How these organisms coordinate
189 the biogenesis of this complex structure to elongate and divide is almost completely
190 unknown.

191 Here, we have studied a highly conserved mycobacterial protein, MSMEG_0317,
192 in Msm and propose to rename it CwdA. As predicted (19), we find that the gene which
193 encodes this protein is essential in Msm. The Mtb homolog*, rv0227c*, is almost certainly
194 essential as well, as no transposon insertions have been found in this gene, even in data
195 sets which combine insertion counts from high density mutagenesis across multiple
196 independent experiments (11).

197 Our data suggest that CwdA's essential function occurs during polar elongation,
198 as cells depleted for CwdA stop elongating, and CwdA-mRFP localizes to the poles.
199 Interestingly, CwdA also localizes to the site of division, yet depleted cells continue to
200 divide. This is consistent with recent work from several groups, which suggests that the
201 essentiality of certain cell envelope structures is different for elongation and division. For
202 example, *C. glutamicum* cells treated with ethambutol, which inhibits the polymerization
203 of arabinan, a core structure in both arabinogalactan and LAM, stop elongating, but
204 continue to divide (25, 26).

205 What is the function of CwdA? Our work suggests that CwdA is involved in the
206 transport of LM/LAM to the outer membrane, either directly or indirectly, and is important

207 for maintaining the structural integrity of the mycobacterial cell envelope. Upon depletion,
208 the levels of several other lipids remain constant or show no reproducible change,
209 suggesting that CwdA may be acting on LM/LAM directly, though our lipid profiling was
210 not exhaustive and we cannot rule out the possibility that another structural lipid is
211 affected by CwdA depletion. However, supporting the notion that CwdA specifically acts
212 upon LM/LAM, we observe a temporal correlation, up until the time of cell lysis, between
213 the accumulation of LM/LAM and the disruption of the envelope. There has been a good
214 deal of speculation as to the localization of LM/LAM in the mycobacterial envelope, but
215 several groups have now shown that at least a fraction of LM/LAM resides in the outer
216 membrane (23, 24). Our data are consistent with a model in which LM/LAM are structural
217 components of the outer membrane. However, mutants of Msm that produce diminished
218 amounts or truncated versions of LM/LAM are viable, suggesting that the presence of
219 LM/LAM in the outer membrane may not be essential for viability (27, 28). Why, then, is
220 *cwdA* essential? We speculate that the accumulation of these large lipoglycans in the
221 periplasm of CwdA-depleted cells causes envelope disruption and cell rupture.

222 One implication from our work is that the transport or correct localization of lipids
223 to the outer membrane is needed for polar elongation, but not division, suggesting that
224 there could be various feedback loops to ensure complete construction of the elaborate
225 mycobacterial cell envelope for insertion of new material to elongate. These checkpoints
226 may be missing during division. This notion is supported by other mutants defective in
227 transporting important outer membrane components like trehalose monomycolate, which,
228 like the *cwdA* mutant, undergo reductive cell division (29).

229 The mycobacterial cell envelope remains an enduring target for the development
230 of new TB therapeutics. The standard TB therapy uses a combination of four drugs; two
231 of these drugs target cell wall synthesis. In addition to the core, and covalently linked
232 structure of peptidoglycan, arabinogalactan, and mycolic acids, the mycobacterial cell
233 envelope is also rich with many other lipids. The functional role of these lipids in bacterial
234 cell physiology is relatively unexplored but they are likely important, if not essential,
235 components of the cell envelope. Our data argue that a more complete understanding of
236 the transport of these molecules could lead to new targets for the development of anti-TB
237 therapeutics.
238
239 **Materials and Methods**
240 **Bacterial strains and culture conditions**: Msm mc^2155 was grown in
241 Middlebrook 7H9 broth supplemented with 0.05% Tween80, 0.2% glycerol, 5 gm/L
242 albumin, 2 gm/L dextrose and 0.003 gm/L catalase or plated on LB agar. *Escherichia coli*
243 DH5α cells were grown in LB broth or on LB agar plates. Concentrations of antibiotics
244 used for Msm is as follows: 20 μg/ml zeocin, 25 μg/ml kanamycin, 50 μg/ml hygromycin,
245 and 20 μg/ml nourseothricin. Concentrations of antibiotics used for *E. coli* used for *E. coli*
246 is as follows: 40 μg/ml zeocin, 50 μg/ml kanamycin, 100 μg/ml hygromycin, and 40 μg/ml
247 nourseothricin.
248 **Plasmids and strains construction:** Before deleting the native copy of
249 *msmeg_0317*, a merodiploid strain was created by inserting a second copy of
250 *msmeg_0317* gene under pTetO promoter using a Kan^R L5 integrating vector.
251 Subsequently, in the merodiploid strain, an in-frame deletion was made by replacing the

252 native copy of *msmeg_0317 gene* with a zeocin resistance cassette flanked by loxP sites
253 using recombineering (18). The plasmid constructs were made using isothermal Gibson
254 assembly whereby insert and vector backbone shared 20-25 bp of homology.
255 *msmeg_0317* and its fluorescent variant were cloned in a Nat^R L5 integrating vector for
256 allele exchange at the L5 site. The *msmeg_0317* depletion strain was made by
257 transforming an episomal Hyg^R marked vector constitutively expressing TetR repressor
258 into a strain expressing a single copy of *msmeg_0317* controlled by the pTetO promoter.
259 mRFP was fused to the c-terminal of *msmeg_0317* gene cloned with 200 bp upstream
260 sequence to capture the native promoter. *ftsZ-mCherry*2B and *eGFP-wag31* genes were
261 cloned under medium strength promoter ptb21 and integrated at tweety (tw) and L5 phage
262 integration sites, respectively.

263 **MSMEG_0317 Depletion:** To transcriptionally deplete *msmeg_0317* in Msm, the
264 ATC-inducible Tet-ON system was used. The only copy of *msmeg_0317* was driven by
265 the pTetO promoter, while the TetR repressor was constitutively expressed in trans from
266 an episomal vector. MSMEG_0317 was depleted by removing ATC from the medium and
267 cells were grown for 18 hours. Subsequently, MSMEG_0317 depleted cells were re-
268 diluted in fresh medium, also without ATC, and samples at different timepoints were taken
269 and processed for cyro-electron microscopy. Alternatively, to avoid changes in LM/LAM
270 abundance that have been found to correlated with cell density and growth phase (21),
271 at 18 hours of depletion, half of the culture was removed for lipid extraction and analysis,
272 and replaced with fresh media. Lipid analysis was performed at timepoints before and
273 after the decrease in OD indicating cessation of growth (Fig. S3).

274 **Time-lapse microscopy**: An inverted Nikon Ti-E microscope was used for the
275 time-lapse imaging. An environmental chamber was maintained at 37°C. Cells were
276 cultivated in an B04 microfluidics plate from CellAsic; continuously supplied with fresh
277 medium; and imaged every 15 minutes using a 1.4 N.A. phase contrast objective.

278 **Kymograph analysis.** Time-lapse images were analyzed in open source image
279 analysis software Fiji (30) and a custom MATLAB program was used to generate
280 kymographs. Specifically, for a single cell, in Fiji, a 5-pixel wide segmented line was drawn
281 from the new pole to the old pole at each time point during the cell cycle. This was
282 repeated on 20-50 cells. These line profiles were then imported into MATLAB, where a
283 custom script was used to generate an average kymograph by 2D interpolation of the
284 individual kymographs.

285 **Lipid extraction and analysis.** Extraction, purification and analysis of lipids were
286 as described previously (31). Briefly, crude lipids were extracted from equal wet cell pellet
287 weights of the MSMEG_0317 depletion strains after 18, 24, 27, 30, and 33 hrs with or
288 without ATC. After lipid extraction using chloroform/methanol, LM and LAM were
289 extracted from the delipidated pellet by incubation with phenol/water (1:1) for 2 hrs at
290 55°C. Phospholipids and PIMs extracted by chloroform/methanol were further purified by
291 *n*-butanol/water phase partitioning, and separated by high performance thin layer
292 chromatography (HPTLC) (Silica gel 60, EMD Merck) using chloroform/methanol/ 13 M
293 ammonia/1 M ammonium acetate/ water (180:140:9:9:23). Phospholipids were visualized
294 via cupric acetate staining. PIMs were visualized with orcinol staining as described (32).
295 LM/LAM samples were separated by SDS-PAGE (15% gel) and visualized using ProQ
296 Emerald 488 glycan staining kit (Life Technologies). To detect LM/LAM in culture

297 supernatants, the supernatants were initially treated with a final concentration of 50 μg/ml
298 Proteinase K for 4 hours at 50°C. The treated supernatants were electrophoresed on 15%
299 SDS-PAGE. LM/LAM were blotted onto nitrocellulose at 20 V for 45 minutes using semi-
300 dry transfer method. Post-transfer, the membrane was blocked by 5% milk in Tris-
301 buffered saline supplemented with 0.05% Tween-20 (TBST). The blocked membrane was
302 then probed overnight with CS-35 antibody (BEI Resources, NIH) at 1:250 dilution at 4°C.
303 The membrane was washed with TBST five times for five minutes each. Post-washing, it
304 was probed with anti-mouse secondary for one hour at room temperature. Membrane
305 was then washed five times for five minutes with TBST. Thermo Scientific's west dura
306 chemiluminescent reagent was used to develop the membrane.

307 **Sample preparation and image collection for Cryo-EM:** Wild type and
308 MSMEG_0317 depleted Msm were pelleted, washed twice with 1X phosphate buffered
309 saline (PBS), and suspended in a very small volume of PBS to get a very dense
310 suspension of bacterial cells. The dense culture was subsequently mixed with 10-nm
311 colloidal gold and deposited onto fresh glow-discharged holey carbon grids. The grids
312 were then blotted with filter paper manually and rapidly frozen in liquid ethane. The frozen
313 grids were transferred under -170 °C into a 300kV Titan Krios equipped with K2 Summit
314 direct detector, a quantum energy filter (Gatan, Pleasanton, CA) and an FEI volta phase
315 plate (FEI). The data was collected using SerialEM (33) and Digital Micrograph
316 software. The motion correction for each movie was done with MotionCor2 (34). The
317 microscope was operated at 300kV with a magnification of 3,600x and 26,000 x for low-
318 mag map and high-mag map respectively. The grey levels of each micrograph are
319 obtained using MATLAB.

Acknowledgements

We thank Cara Boutte and Maikel Boot for helpful suggestions and for critical reading of the manuscript. Work carried out in this manuscript was supported by career award at scientific interface (CASI) from Burroughs Welcome Fund and Searle and Pew funds to E.H.R.

References:

1. **Hoffmann C, Leis A, Niederweis M, Plitzko JM, Engelhardt H.** 2008. Disclosure of the mycobacterial outer membrane: cryo-electron tomography and vitreous sections reveal the lipid bilayer structure. Proc Natl Acad Sci U S A **105:**3963-3967.
2. **Zuber B, Chami M, Houssin C, Dubochet J, Griffiths G, Daffe M.** 2008. Direct visualization of the outer membrane of mycobacteria and corynebacteria in their native state. J Bacteriol **190:**5672-5680.
3. **Jackson M.** 2014. The mycobacterial cell envelope-lipids. Cold Spring Harb Perspect Med **4**.
4. **Jankute M, Cox JA, Harrison J, Besra GS.** 2015. Assembly of the Mycobacterial Cell Wall. Annu Rev Microbiol **69:**405-423.
5. **Kieser KJ, Rubin EJ.** 2014. How sisters grow apart: mycobacterial growth and division. Nat Rev Microbiol **12:**550-562.
6. **Hett EC, Rubin EJ.** 2008. Bacterial growth and cell division: a mycobacterial perspective. Microbiol Mol Biol Rev **72:**126-156, table of contents.
7. **Baranowski C, Rego EH, Rubin EJ.** 2019. The Dream of a Mycobacterium. Microbiol Spectr **7**.
8. **Wu KJ, Zhang J, Baranowski C, Leung V, Rego EH, Morita YS, Rubin EJ, Boutte CC.** 2018. Characterization of Conserved and Novel Septal Factors in Mycobacterium smegmatis. J Bacteriol **200**.
9. **Doerks T, van Noort V, Minguez P, Bork P.** 2012. Annotation of the M. tuberculosis hypothetical orfeome: adding functional information to more than half of the uncharacterized proteins. PLoS One **7:**e34302.
10. **Rego EH, Audette RE, Rubin EJ.** 2017. Deletion of a mycobacterial divisome factor collapses single-cell phenotypic heterogeneity. Nature **546:**153-157.
11. **DeJesus MA, Gerrick ER, Xu W, Park SW, Long JE, Boutte CC, Rubin EJ, Schnappinger D, Ehrt S, Fortune SM, Sassetti CM, Ioerger TR.** 2017. Comprehensive Essentiality Analysis of the Mycobacterium tuberculosis Genome via Saturating Transposon Mutagenesis. MBio **8**.

358 12. **Zhang YJ, Ioerger TR, Huttenhower C, Long JE, Sassetti CM, Sacchettini JC, Rubin**
359 **EJ.** 2012. Global assessment of genomic regions required for growth in Mycobacterium
360 tuberculosis. PLoS Pathog **8:**e1002946.
361 13. **Soltan Mohammadi N, Mafakheri S, Abdali N, Barcena-Uribarri I, Tauch A, Benz R.**
362 2013. Identification and characterization of the channel-forming protein in the cell wall of
363 Corynebacterium amycolatum. Biochim Biophys Acta **1828:**2574-2582.
364 14. **Abdali N, Younas F, Mafakheri S, Pothula KR, Kleinekathofer U, Tauch A, Benz R.**
365 2018. Identification and characterization of smallest pore-forming protein in the cell wall
366 of pathogenic Corynebacterium urealyticum DSM 7109. BMC Biochem **19:**3.
367 15. **Sulzenbacher G, Canaan S, Bordat Y, Neyrolles O, Stadthagen G, Roig-Zamboni V,**
368 **Rauzier J, Maurin D, Laval F, Daffe M, Cambillau C, Gicquel B, Bourne Y, Jackson**
369 **M.** 2006. LppX is a lipoprotein required for the translocation of phthiocerol
370 dimycocerosates to the surface of Mycobacterium tuberculosis. EMBO J **25:**1436-1444.
371 16. **Martinot AJ, Farrow M, Bai L, Layre E, Cheng TY, Tsai JH, Iqbal J, Annand JW,**
372 **Sullivan ZA, Hussain MM, Sacchettini J, Moody DB, Seeliger JC, Rubin EJ.** 2016.
373 Mycobacterial Metabolic Syndrome: LprG and Rv1410 Regulate Triacylglyceride Levels,
374 Growth Rate and Virulence in Mycobacterium tuberculosis. PLoS Pathog **12:**e1005351.
375 17. **Pashley CA, Parish T.** 2003. Efficient switching of mycobacteriophage L5-based
376 integrating plasmids in Mycobacterium tuberculosis. FEMS Microbiol Lett **229:**211-215.
377 18. **van Kessel JC, Hatfull GF.** 2007. Recombineering in Mycobacterium tuberculosis. Nat
378 Methods **4:**147-152.
379 19. **Cashmore TJ, Klatt S, Yamaryo-Botte Y, Brammananth R, Rainczuk AK,**
380 **McConville MJ, Crellin PK, Coppel RL.** 2017. Identification of a Membrane Protein
381 Required for Lipomannan Maturation and Lipoarabinomannan Synthesis in
382 Corynebacterineae. J Biol Chem **292:**4976-4986.
383 20. **Rahlwes KC, Sparks IL, Morita YS.** 2019. Cell Walls and Membranes of Actinobacteria.
384 Subcell Biochem **92:**417-469.
385 21. **Dhiman RK, Dinadayala P, Ryan GJ, Lenaerts AJ, Schenkel AR, Crick DC.** 2011.
386 Lipoarabinomannan localization and abundance during growth of Mycobacterium
387 smegmatis. J Bacteriol **193:**5802-5809.
388 22. **Pitarque S, Larrouy-Maumus G, Payre B, Jackson M, Puzo G, Nigou J.** 2008. The
389 immunomodulatory lipoglycans, lipoarabinomannan and lipomannan, are exposed at the
390 mycobacterial cell surface. Tuberculosis (Edinb) **88:**560-565.
391 23. **Gaur RL, Ren K, Blumenthal A, Bhamidi S, Gibbs S, Jackson M, Zare RN, Ehrt S,**
392 **Ernst JD, Banaei N.** 2015. Correction: LprG-Mediated Surface Expression of
393 Lipoarabinomannan Is Essential for Virulence of Mycobacterium tuberculosis. PLoS
394 Pathog **11:**e1005336.
395 24. **Shukla S, Richardson ET, Athman JJ, Shi L, Wearsch PA, McDonald D, Banaei N,**
396 **Boom WH, Jackson M, Harding CV.** 2014. Mycobacterium tuberculosis lipoprotein
397 LprG binds lipoarabinomannan and determines its cell envelope localization to control
398 phagolysosomal fusion. PLoS Pathog **10:**e1004471.
399 25. **Zhou X, Rodriguez-Rivera FP, Lim HC, Bell JC, Bernhardt TG, Bertozzi CR, Theriot**
400 **JA.** 2019. Sequential assembly of the septal cell envelope prior to V snapping in
401 Corynebacterium glutamicum. Nat Chem Biol **15:**221-231.

402 26. **Schubert K, Sieger B, Meyer F, Giacomelli G, Bohm K, Rieblinger A, Lindenthal L,**
403 **Sachs N, Wanner G, Bramkamp M.** 2017. The Antituberculosis Drug Ethambutol
404 Selectively Blocks Apical Growth in CMN Group Bacteria. MBio **8**.
405 27. **Fukuda T, Matsumura T, Ato M, Hamasaki M, Nishiuchi Y, Murakami Y, Maeda Y,**
406 **Yoshimori T, Matsumoto S, Kobayashi K, Kinoshita T, Morita YS.** 2013. Critical roles
407 for lipomannan and lipoarabinomannan in cell wall integrity of mycobacteria and
408 pathogenesis of tuberculosis. MBio **4:**e00472-00412.
409 28. **Kaur D, McNeil MR, Khoo KH, Chatterjee D, Crick DC, Jackson M, Brennan PJ.**
410 2007. New insights into the biosynthesis of mycobacterial lipomannan arising from
411 deletion of a conserved gene. J Biol Chem **282:**27133-27140.
412 29. **Fay A, Czudnochowski N, Rock J, Johnson JR, Krogan NJ, Rosenberg O, Glickman**
413 **MS.** 2019. Two accessory proteins govern MmpL3 mycolic acid transport in mycobacteria.
414 bioRxiv doi:10.1101/581447**:**581447.
415 30. **Schindelin J, Arganda-Carreras I, Frise E, Kaynig V, Longair M, Pietzsch T,**
416 **Preibisch S, Rueden C, Saalfeld S, Schmid B, Tinevez JY, White DJ, Hartenstein V,**
417 **Eliceiri K, Tomancak P, Cardona A.** 2012. Fiji: an open-source platform for biological-
418 image analysis. Nat Methods **9:**676-682.
419 31. **Rahlwes KC, Puffal J, Morita YS.** 2019. Purification and Analysis of Mycobacterial
420 Phosphatidylinositol Mannosides, Lipomannan, and Lipoarabinomannan. Methods Mol
421 Biol **1954:**59-75.
422 32. **Sena CB, Fukuda T, Miyanagi K, Matsumoto S, Kobayashi K, Murakami Y, Maeda**
423 **Y, Kinoshita T, Morita YS.** 2010. Controlled expression of branch-forming
424 mannosyltransferase is critical for mycobacterial lipoarabinomannan biosynthesis. J Biol
425 Chem **285:**13326-13336.
426 33. **Mastronarde DN.** 2005. Automated electron microscope tomography using robust
427 prediction of specimen movements. J Struct Biol **152:**36-51.
428 34. **Zheng SQ, Palovcak E, Armache JP, Verba KA, Cheng Y, Agard DA.** 2017.
429 MotionCor2: anisotropic correction of beam-induced motion for improved cryo-electron
430 microscopy. Nat Methods **14:**331-332.
431 35. **Larrouy-Maumus G, Gilleron M, Skovierova H, Zuberogoitia S, Brennan PJ, Puzo**
432 **G, Jackson M, Nigou J.** 2015. A glycomic approach reveals a new mycobacterial
433 polysaccharide. Glycobiology **25:**1163-1171.
434
435

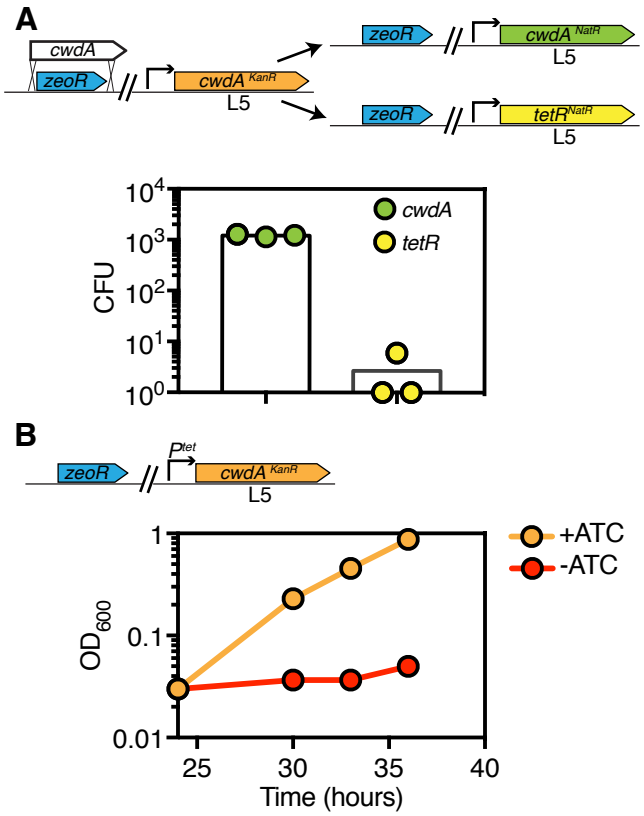

Fig. 1. *cwdA* is essential in Msm. (A) L5-integrating vectors carrying either *cwdA* or a gene encoding TetR were transformed into a strain whose only copy of *cwdA* was at the L5 integration site, and transformants were counted. Bars represent means of biological triplicates and are representative data of three independently performed experiments. (B) Optical density over time of a strain whose only copy of *cwdA* is tetracycline inducible, with and without ATC (+/-ATC). Points are means of three biological replicates. Error bars are too small to be visible. Experiment was performed at least 4 times on separate days, and representative data are shown. ATC=anhydrotetracycline. Time on the *x*-axis corresponds to time after ATC was removed.

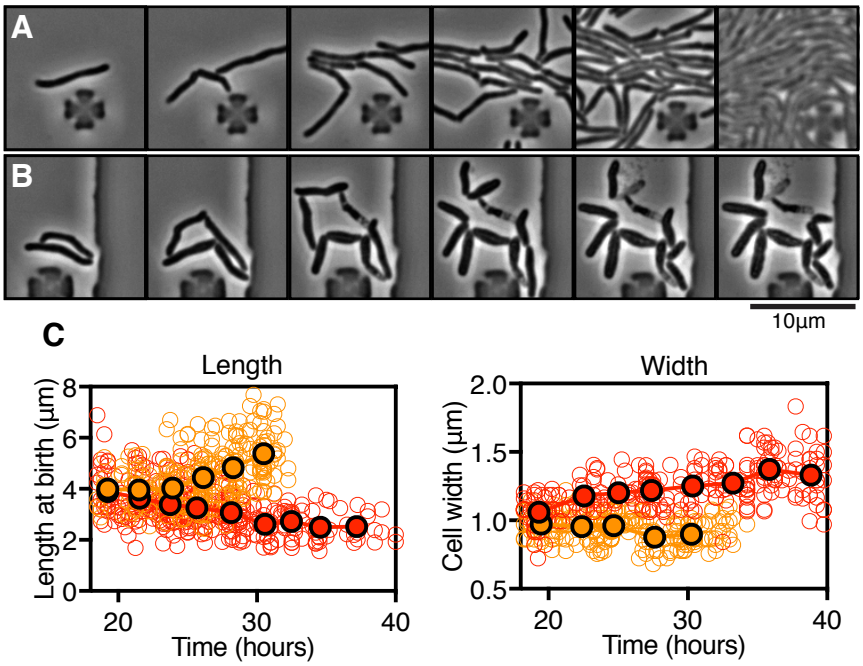

Fig. 2. CwdA-depletion causes reductive cell division and eventual cell lysis. (A,B) The strain shown in Fig. 1B was visualized by time-lapse microscopy in the presence (A) or absence (B) of ATC. Cells were loaded into a microfluidic device 18 hours after the removal of ATC (B) or a mock control (A). Representative frames are 3 hours apart. (C) Birth lengths and cell widths over time of depletion (orange = +ATC; red = -ATC). Open circles represent individual cells (length: N = 261 (length) & 253 (width) for +ATC; N = 355 (length) & 254 (width) -ATC). Closed circles are not fits to the data but represent the mean of cells in 2.25-hr (length) or 2.75-hr (width) bins. The experiment was performed twice on separate days. In +ATC cultures, cell density became too high to measure length and width past ~33 hrs. ATC=anhydrotetracycline

462

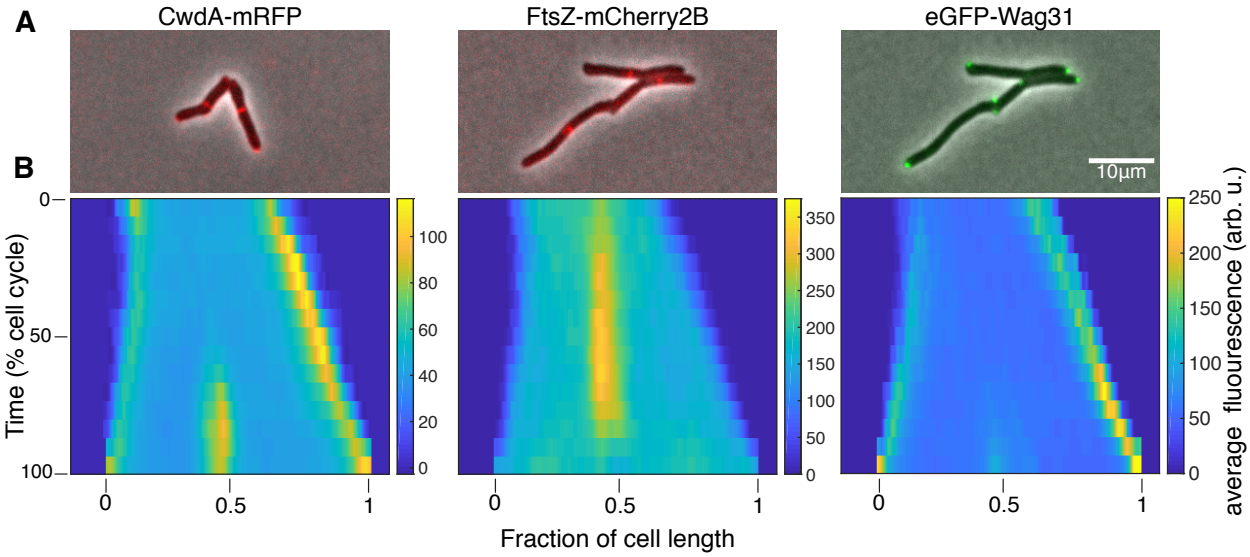

463

464 **Fig. 3. CwdA localizes to the sites of division and elongation**. (A) Merged phase-
465 contrast and fluorescence images of Msm cells expressing CwdA-mRFP, eGFP-Wag31
466 and FtsZ-mCherry2b. (B) Average fluorescent distributions over time (kymographs) from
467 cells aligned from new to old poles and from birth to division (N=20 CwdA-mRFP; N=48
468 FtsZ-mCherry2B; N=20 eGFP-Wag31).

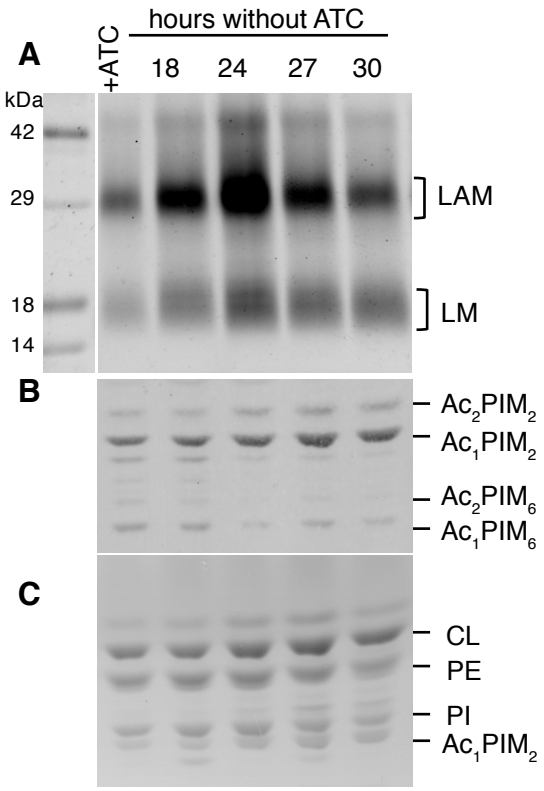

Fig. 4. LM/LAM accumulate as CwdA is depleted. In a strain whose only copy of *cwdA* is ATC-inducible, (A) LM/LAM, (B) non-polar and polar PIMs, (C) and plasma membrane lipids were analyzed by (A) SDS-PAGE and (B-C) TLC during CwdA depletion (without ATC). Cell pellets were normalized by wet weight to account for differences in cell density. Two other biological replicates are shown in Fig. S2. CL, cardiolipin; PE, phosphatidylethanolamine; PI, phosphatidylinositol.

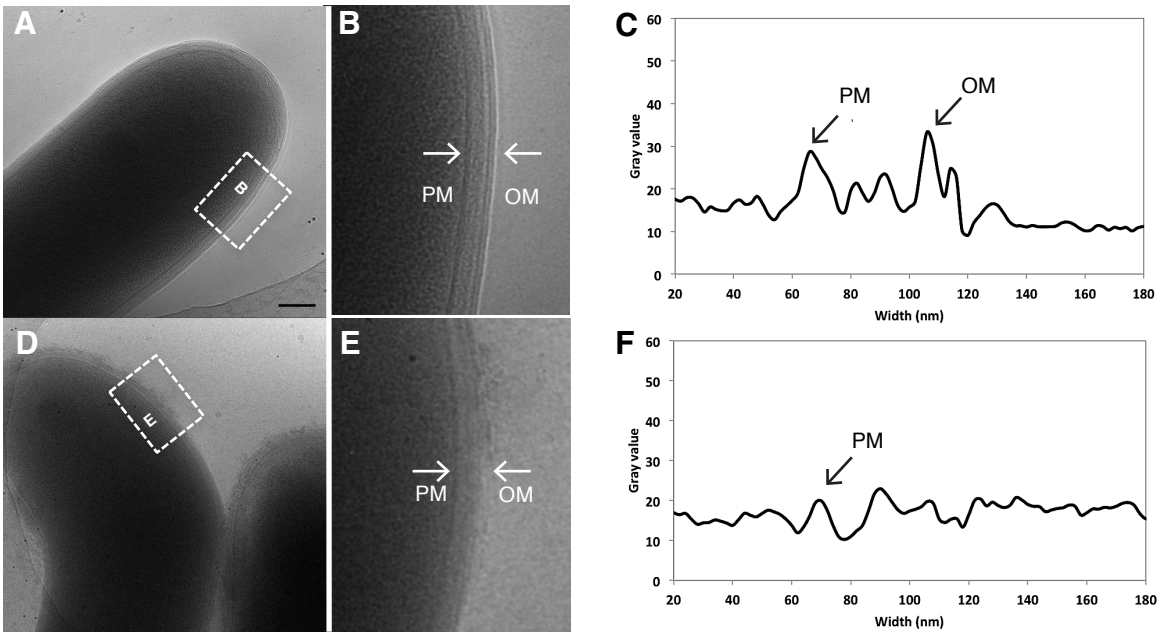

Fig. 5. Depletion of CwdA leads to loss of outer membrane. The cell envelope of a representative wild type Msm cell (A-C) and a cell depleted for CwdA for 24 hours were (D-F) visualized (A,B,D,E), and measured (C,F) by cryo-electron microscopy. PM = plasma membrane; OM = outer membrane. Scale bar = 100 nm.

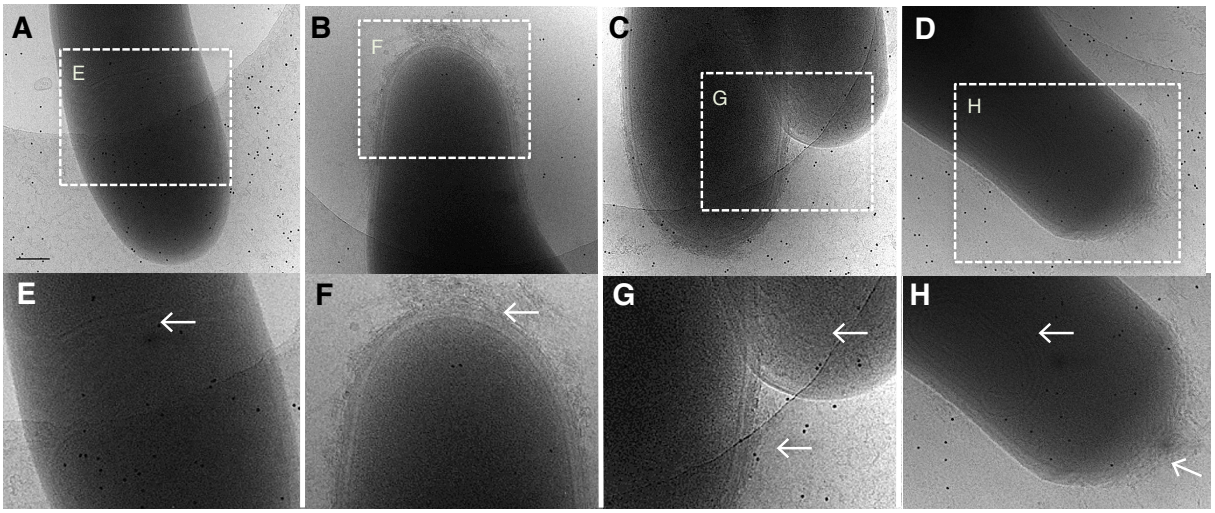

Fig. 6. Cryo-electron microscopy of CwdA-depleted cells (A-H) The cell envelopes of CwdA-depleted cells show plasma membrane invaginations (A&E; C&G; D&H) and outer membrane wall fraying (B-D; F-H) (arrows). (A-C; E-G) 24 hours; (D&H) 33 hours of depletion. Scale bar = 100 nm.

494 **Supplemental Information**

495

496 Figure S1: CwdA-mRFP encodes a functional copy of CwdA

497 Figure S2: Two additional biological replicates of LM/LAM analysis during CwdA depletion

498 Figure S3: Detection of cell-associated and shed LM/LAM during CwdA over-expression

499 Figure S4: An additional biological replicate of cell-associated LM/LAM and other lipids

500 during CwdA over expression

501

502 Movie S1. Cells whose only copy of *cwdA* is ATC-inducible are imaged over time by

503 phase-contrast microscopy in the presence of ATC. Cells were treated in parallel to those

504 shown in Movie S2, except ATC was included in the culture media at all times.

505

506 Movies S2. Cells whose only copy of *cwdA* is ATC-inducible, are imaged over time by

507 phase-contrast microscopy in the absence of ATC. Cells were loaded into the device 18

508 hours after the removal of ATC.

509

510 Table S1: A list of strains used in this study.

Strain	Usage
Mycobacterium smegmatis mc^2 155	Wild type strain, lab stock
mc2 155 L5::pTetO-*cwdA*-kan^R	Merodiploid strain used for deleting native copy of *cwdA*
mc2 155 Δ*cwdA* L5::pTetO-*cwdA*-kan^R	Parental strain used for allele exchange of *cwdA* at L5 site
mc2 155 Δ*cwdA* L5::pTetO-cwdA/pTetR	ATC inducible *cwdA* strain where *cwdA* is under TetO promoter and the strain carries constitutive TetR repressor; used for transcriptional depletion of *cwdA*
mc2 155 Δ*cwdA* L5::pTetO-MS0317-myc/pTetR	ATC inducible C-terminal myc-tagged *cwdA* strain where *cwdA* is under TetO promoter and the strain carries

	constitutive TetR repressor; used for transcriptional depletion of *cwdA*
mc2 155 /pTetOR-*cwdA*-myc	ATC inducible C-terminal myc-tagged *cwdA* strain; used for over-expression of CwdA protein
mc2 155 Δ*cwdA* pL5:pNative-*cwdA*-mRFP-myc	Strain carrying C-terminal mRFP tagged CwdA protein expressed from native promoter to track the localization of CwdA protein
mc2155 L5::pG-MCK-ptb21-egfp-wag31 tweety::ptb21-ftsZ-mCherry2B	Strain used to track the localization of Wag31 and FtsZ proteins (Rego et al 2017, *Nature*)

511

512

513 Table S2: A list of primers used in this study

MS_0317_FP	GCTTAATTAAGAAGGAGATATACATAT GAACCGCGCTGTGGCGCTGCGTATCG	Forward primer to amplify *cwdA* from Msm genome
MS_0317_RP	GGTCCCCAATTAATTAGCTAAAGCTTTC AGATCGGTCGGTCCGGTGGCAGATCG	*Reverse* primer to amplify *cwdA* from Msm genome
MS_0317_1	GGAGCGCAGGTAGTGCCCGGTTCTCG	Forward primer to amplify the upstream region for *cwdA* knock-out construct
MS_0317_2	GGCGTTACCCAACTTAATCGCCTTGCA GCTCACCCCAGAAGTCCACATGCCGCG	Reverse primer to amplify the upstream region for *cwdA* knock-out construct
MS_0317_3	CGCGGCATGTGGACTTCTGGGGTGAGC TGCAAGGCGATTAAGTTGGGTAACGCC	forward primer to amplify zeo^R cassette for

		cwdA knock-out construct
MS_0317_4	GCACCTGGATGCCCTGCGTATCGAA GAAACAGCTATGACCATGATTACGCC	reverse primer to amplify zeo^R cassette for *cwdA* knock-out construct
MS_0317_5	GGCGTAATCATGGTCATAGCTGTTTC TTCGATACGCAGGGCATCCAGGTGC	Forward primer to amplify the downstream region for *cwdA* knock-out construct
MS_0317_6	AGACTCCAGTGGCCCTGCAACAACCGC	Reverse primer to amplify the downstream region for *cwdA* knock-out construct
MS0317_Nat_Fwd	CGATCCGCATGCTTAATTAAG AAGGAGATATACTAATGAACCGCG CTGTGGCGCTGCGT	Forward primer for sub-cloning *cwdA* into L5 integrating pTetO-Nat^R vector
MS0317_Nat_Rev	CCTCTAGGGTCCCCAATTAATT AGCTAAAGCTTTCAGATCGGTC GGTCCGGTGGCAGATCG	Reverse primer for sub-cloning *cwdA* into L5 integrating pTetO-Nat^R vector
MS0317_KO_Fwd	GGATCACGATCACCGCCACCAC GTAGC	Forward sequencing primer to confirm deletion of *cwdA* gene
MS0317_KO_Rev	CCAGAACACCAGCGGAGCCACC GGAGTCC	Reverse sequencing primer to confirm

		deletion of *cwdA* gene
MS0317-Nat_myc-Rev	TCCCCAATTAATTAGCTAAAGCTT TCACAGGTCTTCCTCGCTGATCAGC TTCTGCTCGATCGGTCGGTCCGGTGGC	Reverse primer for attaching myc tag at C-terminus of *cwdA*
pNative317-RFP_1	CGATCCGCATGCTTAATTAAGAAGGAG ATATACTAATGAACCGCGCTGTGGCGCTGCGT	Gibson primers used for making *pNative_ cwdA _mrfp* construct
pNative317-RFP_2	CCTTGATGACGTCCTCGGAGGAGGC CGAGCCGCCGATCGGTCGGTCCGGT GGCAGATCGG	Gibson primers used for making *pNative_ cwdA _mrfp* construct
pNative317-RFP_3	CCGATCTGCCACCGGACCGACCGAT CGGCGGCTCGGCCTCCTCCGAGGACGTCATCAAGG	Gibson primers used for making *pNative_ cwdA _mrfp* construct
pNative317-RFP_4	GGTCCCCAATTAATTAGCTAAAGCTT TCACAGGTCTTCCTCGCTGATC AGCTTCTGCTCGGCGCCGG TGGAGTGGCGGCCCTCGGCGC	Gibson primers used for making *pNative_ ms_0317_mrfp* construct

514

515

516

517 **Supplemental Figures**
518
519

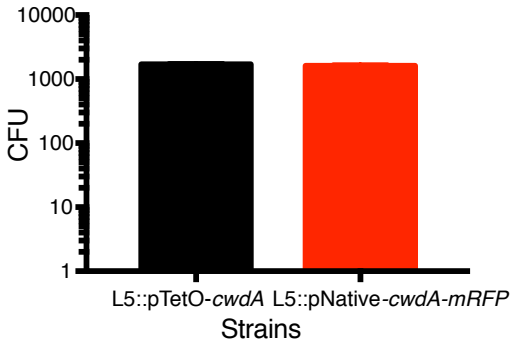

520
521
522
523 **Fig. S1. CwdA-mRFP encodes a functional copy.** L5-allele swapping with *cwdA* or
524 *cwdA-mRFP* expressed by the native promoter. Bars represent means of 3 biological
525 replicates. Error bars indicate standard deviation.
526

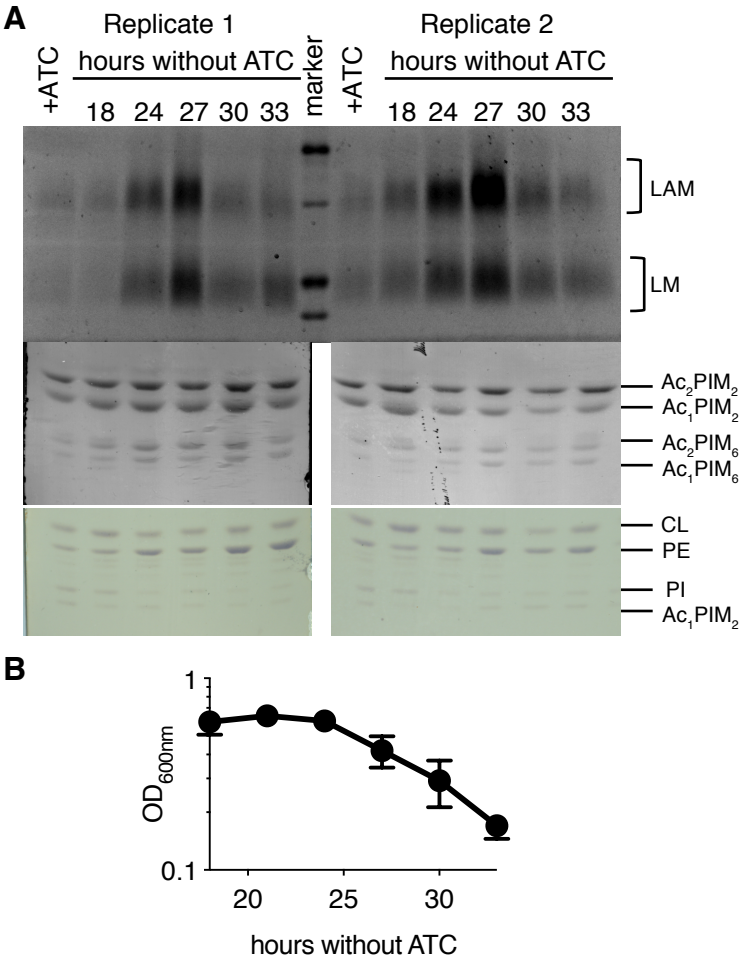

527
528
529 **Fig. S2. Two additional biological replicates of LM/LAM analysis during CwdA**
530 **depletion.** (A) As in Main Text Figure 4, LM/LAM and other lipids were extracted and
531 separated by SDS-PAGE and TLC in cells expressing (+ATC) and depleted for (-ATC)
532 CwdA. Two biological replicates are shown. (B) The optical density of the cultures was
533 measured as CwdA was depleted. To avoid changes in LM/LAM due to cell density, at
534 the indicated timepoints, half of the culture was taken for lipid analysis, and replaced with
535 fresh media. Filled circles indicate means; error bars indicate standard deviation.
536

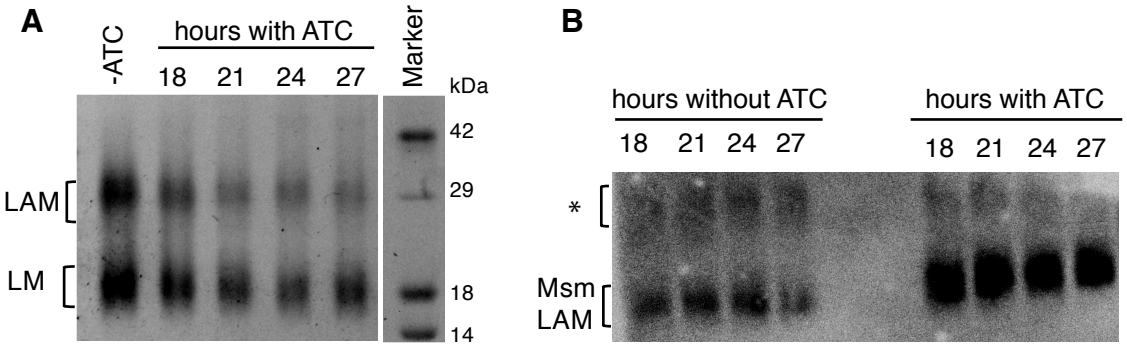

Fig. S3. Detection of cell-associated and shed LM/LAM during CwdA over-expression. In cells carrying an ATC-inducible copy of *cwdA* on a multicopy plasmid, (A) cell-associated LM/LAM were extracted, separated via SDS-PAGE, and visualized by ProQ Emerald with and without ATC. (B) The culture supernatants of those cells were also probed for LAM by western blot using an anti-LAM antibody (CS-35, BEI resources) specific to the arabinan moiety of LAM. The high molecular weight species marked by * likely corresponds to the recently described LAM-like polysaccharide (35).

548
549

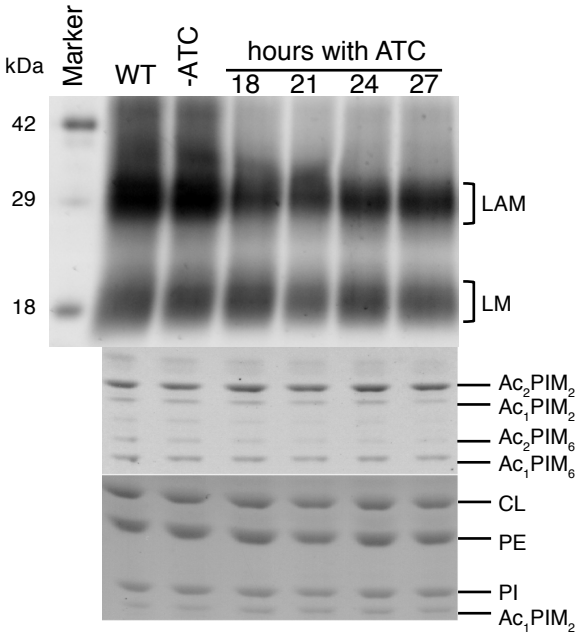

550
551
552
553
554 **Fig. S4. An additional biological replicate of cell-associated LM/LAM and other**
555 **lipids during CwdA over expression.** As in Fig S3, cell-associated were separated
556 and visualized by SDS-PAGE. Other lipids were also separated and visualized by TLC.